Optical Characterization of Solid-State Coextruded PET

T. SUN*, T. KYU,† J. SHENG, D. LEFEBVRE,‡ R. S. STEIN, and ROGER S. PORTER, *Polymer Science and Engineering Department, Materials Research Laboratory, University of Massachusetts, Amherst, Massachusetts 01003*

Synopsis

Amorphous poly(ethylene terephthalate) has been solid state coextruded to a series of draw ratios up to 4.4 at 50, 60, 70 and 90°C. These uniaxially drawn samples have been examined by optical microscopy and light scattering and for increases in crystallinity and birefringence as a function of draw ratio and draw temperature. The birefringence for PET may be among the highest yet reported—0.21.

INTRODUCTION

Poly(ethylene terephthalate) (PET) is the most commercially important polyester. Amorphous PET is of little application due to its brittleness and low strength. However, by drawing under a suitable condition, strong and tough PET can be made. The influence of draw ratio, draw temperature, and deformation rate on crystallinity and orientation upon drawing of amorphous PET have been extensively studied.[1-6] Relatively little work has been reported, however, on the structure of PET drawn below its T_g.[7-11] Stretching of PET below T_g by conventional draw causes necking at low (5%) strain, so the only sample available by such means has the natural draw ratio of about 4.3.

By solid state coextrusion,[12] amorphous PET film has been drawn in this laboratory to a series of constant draw ratios, without neck formation and at temperature below T_g.[13,14] The purpose of the present study is to investigate the PET superstructure in a series of these uniformly drawn films prepared both below and above T_g as a function of extrusion draw ratio and temperature using small-angle light scattering, polarized optical microscopy, birefringence and crystallinity measurements, so that the morphology development in the course of draw can be revealed.

* On leave from East China Institute of Textile Science and Technology, Shanghai, People's Republic of China.

† Polymer Engineering Center, University of Akron, Akron, OH.

‡ 15 Bd, Heri 4 75004, France.

Journal of Applied Polymer Science, Vol. 30, 251-262 (1985)
 CCC 0021-8995/85/010251-12$04.00

EXPERIMENTAL

Sample

A PET film with thickness of 25 μm was used. It was virtually amorphous ($\leq 2\%$ crystallinity) and isotropic by density and birefringence. The molecular weight $\overline{M}_n$ was about 14,500.*

Coextrusion

The PET film was deformed by the split billet coextrusion technique in an Instron Capillary Rheometer according to the procedure reported previously.[13,14]

Crystallinity

Crystallinity was measured by a density gradient column using a carbon tetrachloride–heptane mixture at 25°C. The crystallinity (volume fraction) X_v, was calculated from a two-phase model,[13,14] assuming a crystal density d_c of 1.455 and an amorphous density d_a of 1.335 g/cm^3 as follows:

$$d = d_c X_v + d_a(1 - X_v)$$

Here, d represents the sample density.

Birefringence

The birefringence of various PET films was measured by using a Rotatable Compensator with quartz combination plates. White light, considered to be 550 nm, was used as a source.

Small Angle Light Scattering

Small-angle light scattering of all PET deformates was investigated using the conventional photographic technique reported previously.[11,15–18] Scattering patterns (V_v, H_h, and H_v) were obtained with the analyzer and the polarizer parallel and perpendicular, respectively. The drawing direction is always taken as vertical. The light source was an He–Ne gas laser with a wave length of 6328 Å and a power of 0.5 mW.

To quantitatively analyze the small-angle light scattering (SALS) patterns, an optical multichannel analyzer (OMA2) has also been used. This apparatus, developed in our laboratory, has been described.[19] However, it appears useful to describe briefly the procedure for quantitative analysis. The data are collected using a vidicon detector and its controller (Princeton Applied Research Corp.) and transmitted to microprocessor (LSI 11/2, 64K byte RAM, Digital Equipment Corp.). For each pattern 40 $\times$ 40 points have been saved; each point is an average of 10 $\times$ 10 points of the vidicon detector x-y strid. The data are stored on floppy disks and analyzed using the microcomputer facilities. The system is calibrated in absolute intensity using

* The cast amorphous PET used in this study was prepared and kindly provided by Dr. C. J. Heffelfinger, E. I. DuPont de Nemours and Co., Inc., Circleville, Ohio.

a calibrated opal glass diffuser as described.[20] The calibration in polar scattering angle is obtained by recording the SALS diffraction pattern from a line grating. Using this dual calibration and with a knowledge of sample thickness, the absolute intensities (Rayleigh factors) can be calculated. To increase the precision, a quadrant averaging has been made using the microcomputer. By using the microprocessor, the evolution of the intensity can also be plotted in function of the scattering angle for a value of the azimuthal angle which corresponds to the intensity maximum.

To further evaluate interpretations based on SALS, polarized micrographs have also been obtained.

RESULTS

Crystallinity

The crystallinity of the starting PET remains low and fairly constant up to an extrusion draw ratio (EDR) of 2.0 regardless of the temperature of drawing, above, below or near T_g. The crystallinity increases sharply as EDR exceeds 2.0. This suggests that extensive stress-induced crystallization has taken place even at such low temperatures below its T_g. The crystallinity is somewhat greater for drawing at low temperature. This is consistent with a higher stress level resulting in more stress-induced crystallization. The trend reverses above an EDR of 3.4 with crystallinity levelling off with further drawing.

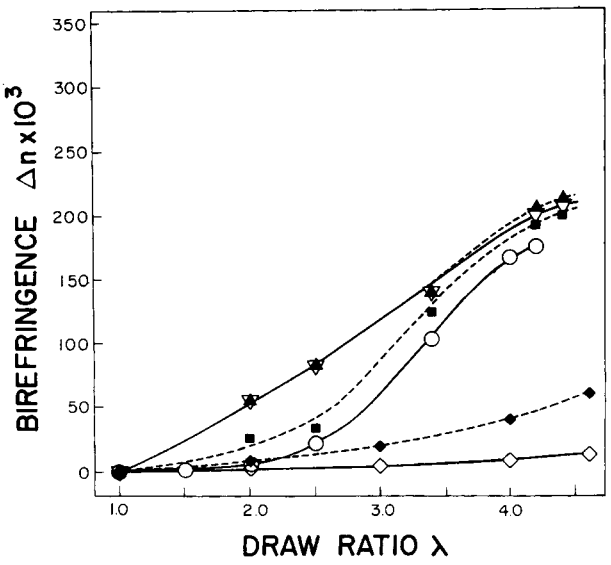

Fig. 1. The variations of birefringence of PET films with respect to extrusion draw ratio for various extrusion temperatures. ET ($\bar{M}_n$ = 14,500)(°C): (▲) 50; (▽) 60; (■) 70; (○) 90. DT(90°C): (◆) $\bar{M}_w$ = 48,000 (◇) $\bar{M}_w$ = 14,000.

Birefringence

Figure 1 shows birefringence of the PET as a function of EDR. The birefringence is influenced by the stress-induced crystallization as well as the orientation of the amorphous and crystalline regions. Significant differences can be noticed for drawing below and above the T_g. At an EDR up to 2.0, the birefringence increases appreciably for draw below T_g. This is primarily due to the orientation of the amorphous matrix since the crystallinity does not appreciably increase. The birefringence does not increase on drawing at 90°C. Above an EDR of 2.0, the birefringence increases rather sharply for low temperature drawing, suggesting that stress-induced crystallization has taken place extensively. On draw at 90°C, the marked increase in birefringence is seen only when EDR exceeds 3.4. Since the crystallinity also increases appreciably, it is believed that the stress-induced crystallization is occurring. Our maximum birefringence of 0.21 in Figure 1 exceeds the previously reported high of 0.17 for PET with a theoretical limit of 0.236[23]. However, we cannot completely define structure completely from density and birefringence data alone. We thus turned to the small-angle light scattering studies for more detailed information.

Light Scattering

Polarized light scattering photographs obtained under H_v (crosspolarizers) conditions for various draw ratio of 2.0–4.4 are depicted in Figures 2(a)–(b)

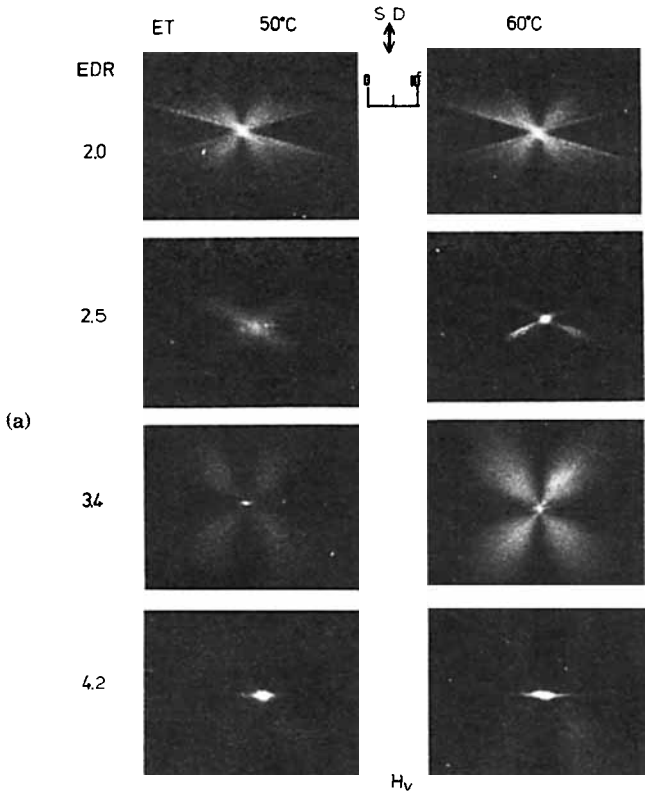

Fig. 2. H_v (crosspolarizers) polarized light scattering photographs of PET films for various extrusion draw ratios and temperatures: (a) 50 and 60°C; (b) 70 and 90°C.

at several drawing temperatures below (50°C, 60°C), about (70°C), and above (90°C) the T_g of the PET. The H_v scattering patterns for 50°C and 60°C are similar for all extrusion ratios. Below an EDR of 2.0, no observable structure is developed, above which cross pattern characteristics of rodlike scattering appear. This suggests that orientational crystallization takes place at an EDR of 2.0–2.4. Upon further draw, the pattern changes to four-lobe clover, somewhat elongated in the draw direction. This four-lobe clover pattern is consistent with a sheaf or ellipsoidal spherulite texture. In addition, a four-streak pattern near the equitorial region is often observed. Similar patterns are also observed in row-nucleated polybutene-1[21] and recently in drawn PET.[11] According to these authors,[11] the four-streak pattern arises from interparticle interference of the assembly of sheaf structures overgrown on row of nuclei.

Similar structural development is also observed on draw at 70°C. At 90°C, no pattern is present below EDR of 2.5. A rodlike scattering pattern is seen at a higher extrusion ratio of 3.5. The V_v and H_h patterns are compared with the H_v patterns in Figure 3. The H_v scattering depends primarily on anisotropy of the rod and orientation fluctuation, while V_v and H_h scattering depend also on an additional factor, i.e., the density fluctuation. Since the scattering arising from the density fluctuation is isotropic in origin, it therefore should not depend on polarization. Hence, if the scattering arises solely from the density fluctuation, the V_v and H_h patterns should be identical. The disimilarity of the V_v and H_h scattering patterns suggests that the

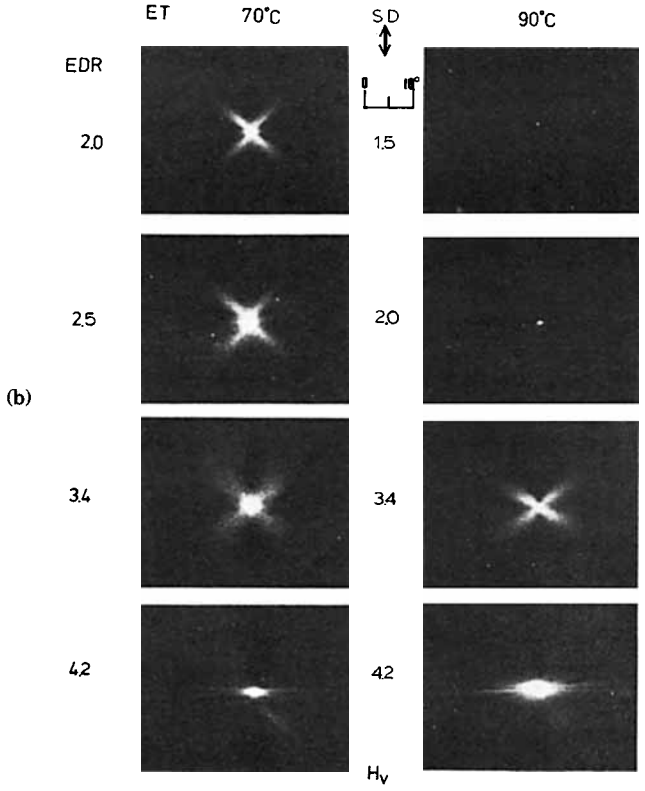

Fig. 2. (*Continued from the previous page.*)

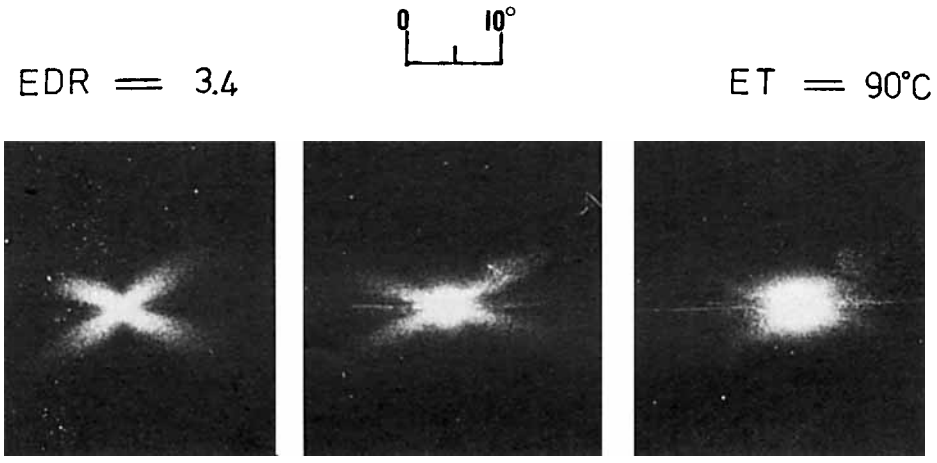

Fig. 3. (a) H_v, (b) V_v, and (c) H_h light scattering patterns of PET film coextruded to a draw ratio of 3.4 at 90°C.

orientation and anisotropy contributions are dominant over density fluctuations. In the case of V_v scattering, polarization is parallel to the draw direction and thus to the molecular chain axis, so that the orientation and anisotropy contributions are relatively large. The contributions of H_h scattering are relatively less; therefore, scattering predominantly arises from density fluctuations. In short, these crystalline PET rods are preferentially oriented at an angle to the draw direction. As before, this rodlike scattering pattern transforms to four-lobe clover superimposed on four-streak in the lateral direction upon further drawing. From photographic light scattering alone it is rather difficult to identify the origin of the four-lobe clover and the four-streak scattering pattern, requiring more quantitative light scattering studies by the 2-dimensional Optical Multichannel Analyzer (OMA-2) developed in this laboratory.[19]

The OMA-2 scans were conducted on PET drawn at 70°C. The H_v quadrant average isointensity contours are shown in Figures 4(a) and (b), in comparison with the slice average of intensity vs. scattering angle obtained at a maximum azimuthal angle (μ_{max}). A beam stop is used to prevent the videcon camera from detecting the strong and intense transmitted light, the effect of which can be seen at the lower corner of the left-hand side of the isointensity contours. These quadrant average contours are reminiscent of the H_v photographs shown in Figure 4(b).

At low level of strain (ERR = 2.5), the contour pattern shows no maximum in the plot of scattered intensity vs. scattering angle which is characteristic of rodlike scattering. At EDR of 3.5 the contour pattern looks similar to a four-lobe clover, but the intensity does not show a clear maximum with respect to scattering angle. Perhaps this arises from incomplete sheaf structure which may be an intermediate structure between a rod and a spherulite. Upon further draw, a clear maximum is seen in the quadrant average isointensity contour and also in the intensity versus scattering angle plot.

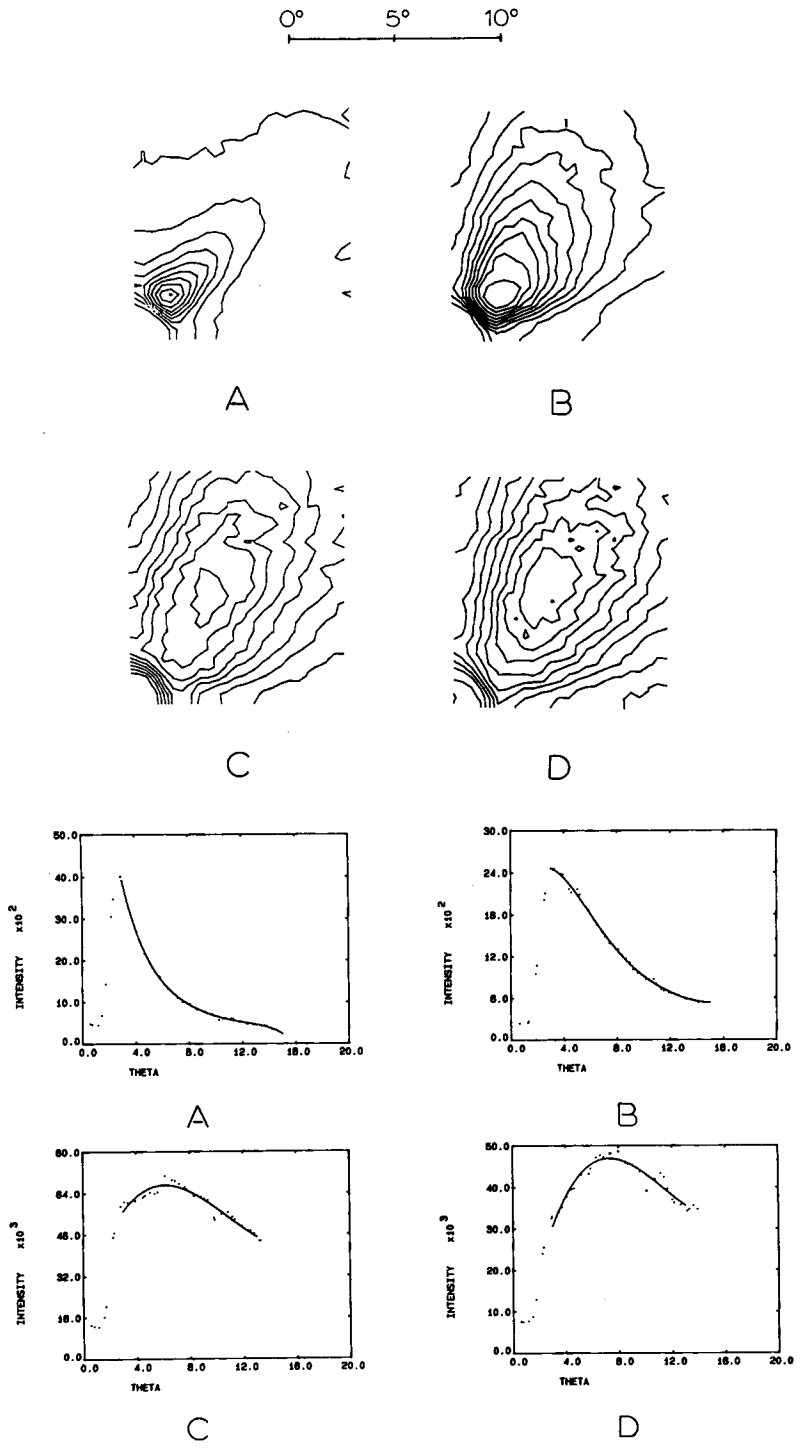

Fig. 4. *Top*: Quadrant average isointensity contours of H_v light scattering patterns of PET film drawn at 70°C for various draw ratios. *Bottom*: Slice average scattered light intensity vs. scattering angle at a maximum azimuthal angle.

The pattern is somewhat elongated in the draw direction which suggests that ellipsoidal spherulites are formed with long axis perpendicular to the direction of extrusion. The radius of the ellipsoid is ca. 3.6–3.9 μm as estimated in accordance with Samuel's equation. The lateral streak pattern is sometimes not clear, however, it is distinct in the case of ET = 90°C. This will be detailed later. A crude conclusion regarding the structural development during orientation crystallization as revealed by light scattering is the formation of rodlike texture which transforms to sheaf structure, and subsequently to ellipsoidal spherulites. The differentiation between sheaf and spherulitic structure is rather difficult by light scattering. The OMA-2 scans have been also conducted on various drawn PET extruded at various temperatures (see Fig. 5 for low draw ratio and Fig. 6 for high draw level).

Optical Microscope

Dark-field optical micrographs, corresponding to photographic light scattering patterns obtained for various drawing temperature and extrusion ratio, are displayed in Figures 7(a) and (b). In agreement with the light scattering studies, a rodlike texture with preferential orientation with re-

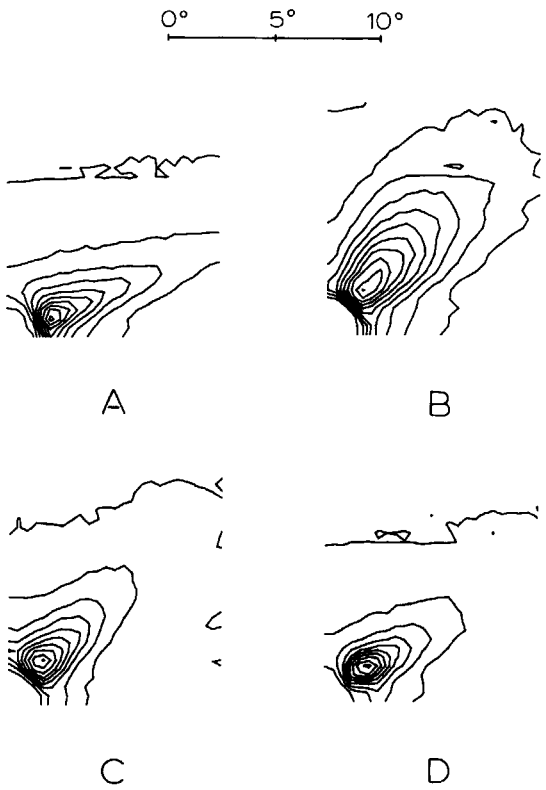

Fig. 5. Quadrant average isointensity contours of H_v light scattering patterns of PET film at low draw ratios for various temperatures: (A) 50°C; (B) 60°C; (C) 70°C; (D) 90°C.

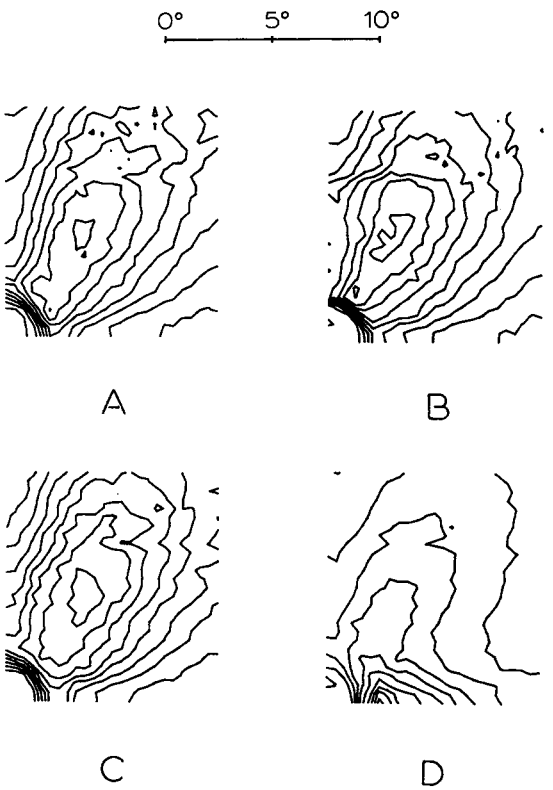

Fig. 6. Quadrant average isointensity contours of H_v light scattering patterns of PET film at high draw ratios for various temperatures: (A) 50°C; (B) 60°C; (C) 70°C; (D) 90°C.

spect to the extrusion direction is observed for samples of low strain. At higher EDR, entities, presumably spherulites, can be seen. The estimated radius is of the order of 3.2 μm, although the size is difficult to evaluate from the micrographs. The shape is somewhat elliptical with long axis perpendicular to the extrusion direction. There is a tendency for the superstructure to be aligned along the drawing direction probably overgrown on row of nuclei. However, the system is not volume-filled by these superstructures since their population (volume fraction) is rather low. Therefore, although the light scattering and optical microscopic studies indicate the existence of these superstructures, they are not the representative of the entire system.

DISCUSSION

A unique feature in this study is the ductility achieved in PET below its T_g, without macroscopic necking. This is due to the characteristics of the solid state coextrusion technique in which every point of the polymer in the extrusion die is evenly subjected to the applied stress, in an extensional flow field which differs from conventional tensile drawing where stress concentration occurs at weak positions leading to necking. It is thus intriguing to learn that crystallization can take place under high stress even

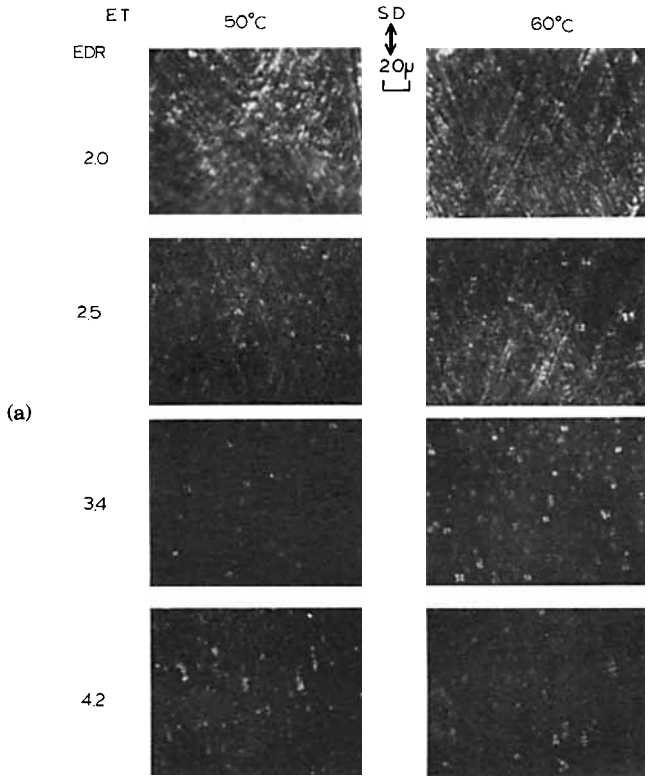

Fig. 7. Dark-field optical micrographs of PET films for several draw ratios and at several temperatures: (a) 50 and 60°C; (b) 70 and 90°C.

at such low temperatures, below the T_g of the undrawn PET. The physics behind this is still unclear.

A crude conclusion regarding the structural development during orientational crystallization as revealed by light scattering is the formation of rodlike texture which advances to a sheaf texture, and subsequently to an ellipsoidal spherulite. This kind of structural development has been observed by thermal crystallization of undrawn PET by Misra and Stein[11] and on PTFE by Rhodes and Stein.[22]

The tendency of alignment of these superstructures (sheaf or ellipsoidal spherulitic) parallel to the extrusion direction exists as demonstrated by the light scattering and the optical micrographs. According to Hashimoto et al. and Matsuo et al., the interparticle interference effect of the assembly of superstructures gives rise to lateral four-streak patterns. However, such a pattern sometimes is not observed here. One possibility to account for this discrepancy is that the system is not volume-filled by these superstructures in our case, although we do confirm that such a tendency of assembly of superstructures does exist.

Another interesting feature is that isolated or assemblies of superstructures (ellipsoidal spherulite) are dispersed in the amorphous matrix, which suggests that amorphous material may exist interspherulitically as well as

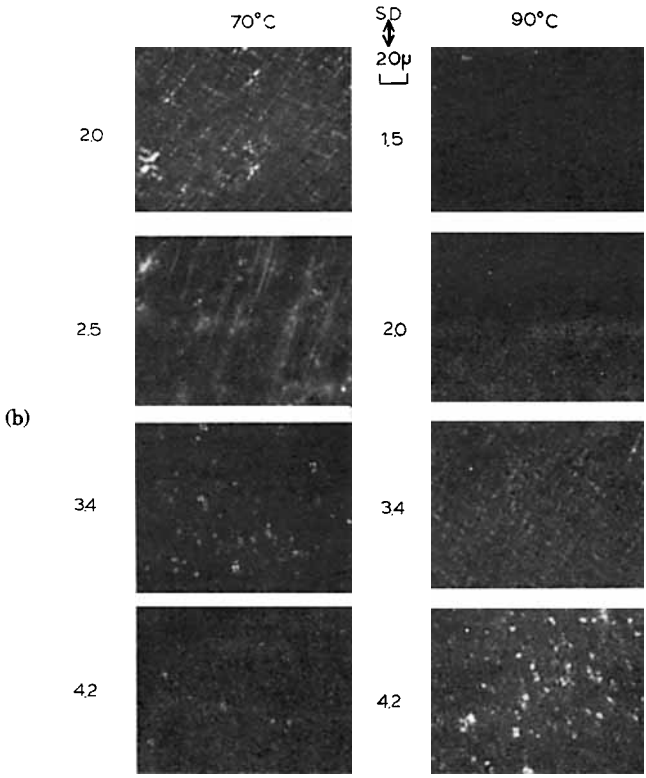

Fig. 7. (*Continued from the previous page.*)

intraspherulitically. Due to the difference in mobility, depending upon location, sometimes dual T_g loss peaks are observed in the dynamic mechanical studies. The degree of crystallinity of the highly drawn PET is the order of 30%. However, the population of the superstructure is considerably low; hence, there is a possibility that crystalline materials may exist outside the superstructure, probably interconnected with the amorphous matrix.

References

1. A. B. Thompson, in *Fiber Structure*, J. W. S. Hearle and R. H. Peters, Eds., Butterworth, Washington, D.C., 1963.
2. A. B. Thompson and I. Marshall, *Proc. Roy. Soc. London, Ser. A*, **211**, 541 (1951).
3. A. B. Thompson and I. Marshall, *J. Appl. Chem.*, **4**, 145 (1954).
4. A. B. Thompson, *J. Polym. Sci.*, **34**, 741 (1959).
5. J. E. Spruiell, D. E. McCord, and R. A. Beuerlein, *Trans. Soc. Rheol.*, **16**(3), 535 (1972).
6. R. P. Sheldon, *Polymer*, **4**, 213 (1963).
7. S. Newman, *J. Polym. Sci.*, **27**, 583 (1963).
8. P. R. Blakey and R. P. Sheldon, *J. Polym. Sci., Part A*, **2**, 1043 (1964).
9. G. E. Wilkes and C. M. Chu, *Am. Chem. Soc., Polym. Prepr.*, **14**(2), 1282 (1973).
10. T. Asano and T. Seto, *Polym. J.* (Jpn.), **5**, 72 (1973).
11. A. Misra and R. S. Stein, *J. Polym. Sci., Polym. Phys. Ed.*, **17**, 235 (1979).
12. P. D. Griswold, A. E. Zachariades, and R. S. Porter, paper presented at Stress-Induced Crystallization Symposium, Midland Macromolecular Institute, Mich., August 1977.
13. J. R. C. Pereira and R. S. Porter, *J. Polym. Sci., Polym. Phys. Ed.*, **21**, 1133 1147 (1983).

14. T. Sun, J. R. C. Pereira, and R. S. Porter, *J. Polym. Sci., Polym. Phys. Ed.*, to appear.
15. M. B. Rhodes and R. S. Stein, *J. Appl. Phys.*, **31**, 1873 (1960).
16. R. J. Samuels, *J. Polym. Sci., A-2*, **9**, 2165 (1971).
17. G. C. Adams, *J. Polym. Sci., A-2*, **6**, 31 (1968).
18. M. B. Rhodes, PhD thesis, University of Massachusetts, 1962.
19. R. J. Tabar, R. S. Stein and M. B. Long, *J. Polym. Sci., Polym. Phys. Ed.*, **20**, 2041 (1982).
20. T. P. Russell, J. Koberstein, R. Prud'homme, A. Misra, R. S. Stein, J. W. Parsons, and R. L. Rowell, *J. Polym. Sci., Polym. Phys. Ed.*, **16**, 1879 (1978).
21. R. S. Stein and A. Misra, *J. Polym. Sci., Polym. Phys. Ed.*, **18**, 327 (1980).
22. M. B. Rhodes and R. S. Stein, *J. Polym. Sci.*, **62**, 587 (1962).
23. A. Wlochowicz, S. Rabiej and J. Janicki, *J. Appl. Polym. Sci.*, **28**, 1335 (1983).

Received January 20, 1984
Accepted September 11, 1984